

Tensile Characteristics of Fiber-Reinforced Cementitious
Composite with Recycled Carbon Fiber

LI SICONG

(Master's Program in Engineering Mechanics and Energy)

Advised by Toshiyuki Kanakubo

Submitted to the Graduate School
of Science and Technology
Degree Programs in Systems and
Information Engineering
in Partial Fulfillment of the Requirements
for the Degree of Master of Engineering
at the University of Tsukuba

March 2024

Abstract

This research aims to investigate the tensile characteristics of fiber-reinforced cementitious composites (FRCC) incorporating recycled carbon fiber. Given the increasing generation of waste from carbon fiber-reinforced polymer (CFRP), recycled carbon fiber presents an effective utilization method. Incorporating fibers into cementitious composites can effectively enhance the mechanical properties of the composites. This study conducts four-point bending tests and uniaxial tension tests on FRCC with recycled carbon fiber. The bending tests confirm that solvolysis method recycled carbon fiber exhibits good mechanical performance in FRCC compared to other recycled carbon fibers. The deflection hardening property of FRCC is observed, and the optimum fiber volume fraction of 0.5% is identified. The bridging law is calculated based on the results of the uniaxial tension tests. A bi-linear stress-strain model is established for the section analysis based on the bridging law. The analytical maximum bending moment shows consistency with the experimental results.

Contents

Chapter 1 Introduction	1
1.1 Research Background	1
1.2 Recycling Methods of Carbon Fiber	2
1.3 FRCC with Carbon Fiber	3
1.4 Tested Recycled Carbon Fiber	4
1.5 Research Objective	5
Chapter 2 Bending Test	6
2.1 Bending Test with 40 mm Cross-section	6
2.1.1 Experiment Overview	6
2.1.2 Compression Test Results	10
2.1.3 Bending Test Results	14
2.2 Bending Test with 100 mm Cross-section	18
2.2.1 Experiment Overview	18
2.2.2 Compression Test Results	21
2.2.3 Bending Test Results	22
2.3 Experimental Conclusion	25
Chapter 3 Uniaxial Tension Test	26
3.1 Experiment Overview	26
3.1.1 Used Materials	26
3.1.2 Specimens	28
3.2 Test Results	30
3.2.1 Compression Test	30
3.2.2 Uniaxial Tension Test	32
Chapter 4 Modeling of Bridging Law	37
4.1 Bridging Law	37
4.2 Section Analysis for Bending Test	41
Chapter 5 Conclusion	45
Acknowledgements	46
Reference	47

List of Figures

Fig. 1.1 Photo of used fiber.....	4
Fig. 2.1 Universal testing machine	8
Fig. 2.2 Four-point bending test with 40 mm cross-section	8
Fig. 2.3 Stress-strain curves of compression test.....	12
Fig. 2.4 Bending specimen after loading	15
Fig. 2.5 Bending moment-curvature curve	16
Fig. 2.6 Four-point bending test with 100 mm cross-section	19
Fig. 2.7 Stress-strain curves of compression test.....	21
Fig. 2.8 Bending moment-curvature curve	23
Fig. 3.1 Electronic system universal testing machine.....	27
Fig. 3.2 Dimensions of specimen for uniaxial tension test (Unite: mm).....	28
Fig. 3.3 The mold for the test specimens	29
Fig. 3.4 Stress-strain curves of compression test.....	31
Fig. 3.5 Tensile load-head displacement relationship.....	33
Fig. 3.6 Photos of specimens after loading	35
Fig. 4.1 Individual fiber bridging model.....	40
Fig. 4.2 Calculation result of bridging law	40
Fig. 4.3 Stress-strain model for section analysis.....	42
Fig. 4.4 Stress distribution in cross-section at the maximum moment	44

List of Tables

Table 2.1 Mix proportion of FRCC	7
Table 2.2 List of specimens	9
Table 2.3 Average compressive strength and elastic modulus	11
Table 2.4 List of maximum bending moment.....	17
Table 2.5 List of specimens	19
Table 2.6 Mix proportion of FRCC	20
Table 2.7 Results of compression test.....	21
Table 2.8 List of maximum bending moment.....	24
Table 3.1 Mix proportion of FRCC	26
Table 3.2 Mechanical properties of fiber	27
Table 3.3 List of the specimens	28
Table 3.4 Results of compression test.....	30
Table 3.5 Results of the uniaxial tension test	36
Table 4.1 Calculation procedure of bridging law	39
Table 4.2 List of maximum bending moment.....	43

Chapter 1 Introduction

1.1 Research Background

In recent years, the huge demand for carbon fiber-reinforced polymer (CFRP) presents serious challenges for the environment. Incorporating of recycled carbon fibers into cementitious composites is an efficient way to use the CFRP waste. Application of recycled carbon fibers can bring beneficial properties to the waste and add significantly improved properties to cementitious composites. Fiber-reinforced cementitious composite (FRCC) is a material which is mixed with short fibers. The tensile characteristics of FRCC after first cracking are significantly influenced by the crack bridging performance of fiber, typically represented by a tensile stress-crack opening relationship known as the bridging law ^[1]. According to the bridging law, its tensile strength and crack resistance can be enhanced.

1.2 Recycling Methods of Carbon Fiber

In recent years, various research on CFRP waste recycling technologies have been carried out. At present, the main recycling methods can be categorized into four types, which are pyrolysis method, solvolysis method, mechanical method and electrochemical method.^[2] In the pyrolysis method, the fiber waste is subjected to high temperatures, approximately 600 Celsius degrees, to degrade the matrix. Furthermore, at a commercial scale, the recycling of carbon fiber is exclusively facilitated through the pyrolysis technique. The solvolysis method uses various chemical solvents to decompose the resin matrix, and recover the remaining carbon fiber, which remains undamaged, and its performance is preserved. The mechanical method is to clean and remove impurities from the CFRP waste and then pulverize and sieve it to obtain powdery resin products and carbon fibers. The electrochemical method is to use electrolysis to recycle CFRP waste. Among them, pyrolysis and solvolysis methods have enormous potential for development because of their high efficiency and strength retention.

1.3 FRCC with Carbon Fiber

Carbon fiber (CF) is one of the most commonly used fibers as fiber-reinforced polymer (FRP). Carbon fiber has a higher elastic modulus and tensile strength than other fibers. FRCC with carbon fiber can be expected to significantly improve tensile performance of FRCC. In past research on fiber-reinforced cementitious composites, under appropriate fiber volume fractions, FRCC has demonstrated well flexural performance. Simultaneously, the inclusion of carbon fibers has also elevated the tensile strength of FRCC. The addition of carbon fiber is more efficient in improving the flexural strength as compared to the uniaxial tensile strength.^[3] However, due to cost considerations, the widespread implementation of carbon fiber in FRCC remains challenging.

1.4 Tested Recycled Carbon Fiber

The pyrolysis (CF-PY) and the solvolysis (CF-SO) are major methods for recycled carbon fiber. In this study, carbon fiber recycled by these two methods are used. Virgin fiber (CF-V) is also used for comparison with recycled fibers. Fig. 1.1 shows fibers by ordinary photograph and scanning electron microscope (SEM) ^[4]. The fibers cut in 10mm length are used for fabrication of FRCC in the case of CF-V and CF-SO. Due to the superior mechanical performance and dispersion characteristics demonstrated by the solvolysis method in recycled carbon fiber compared to other recycling methods (Chapter 2), further investigation into the recycled carbon fibers by solvolysis method is conducted in uniaxial tension tests (Chapter 3).

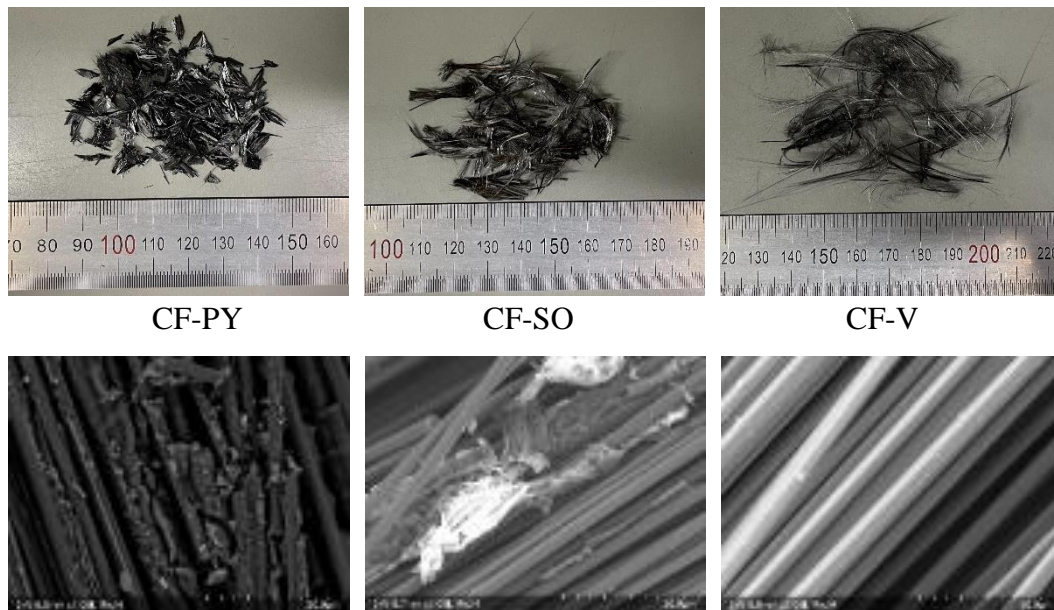


Fig. 1.1 Photo of used fiber

1.5 Research Objective

The objective of this study is to investigate the tensile characteristics of FRCC with recycled carbon fiber by solvolysis method.

In Chapter 2, through bending tests, the appropriate type of recycled carbon fibers and the corresponding fiber volume fractions are identified.

In Chapter 3 and Chapter 4, uniaxial tension tests are performed on specimens with recycled carbon fiber by solvolysis method. The bridging model is established through uniaxial tension test results, and its validation is carried out using the previous bending test results.

Chapter 2 Bending Test

2.1 Bending Test with 40 mm Cross-section

2.1.1 Experiment Overview

The mix proportion of FRCC is shown in Table 2.1. Three distinct types of carbon fiber are utilized in the study. Virgin fiber (CF-V) is used for comparison. The fiber volume fractions are set at 0.5% and 2%. The length of the fiber is controlled at 10 mm. High early strength Portland cement is used to ensure that the target matrix strength is achieved in the early phase of curing. The fiber is added in two stages to facilitate better fiber dispersion. The specimens were covered with plastic wrap for curing in room environment. The demolding of the test specimens is conducted on the seventh day after casting.

As shown in Fig. 2.1, a universal testing machine with a loading capacity of 500kN is used in the test. The uniaxial compression test and four-point bending test are carried out by $\phi 50 \times 100$ mm cylinder and $40 \times 40 \times 160$ mm rectangle test pieces, respectively. In the bending test, axial deformations are measured to calculate the curvature as shown in Fig. 2.2. The list of the specimens is shown in Table 2.2. Six specimens for compression test and six specimens for four-point bending test were prepared for each type of fiber including specimens without fiber (Specimen N).

Table 2.1 Mix proportion of FRCC

Specimen	Unit weight (kg/m ³)					
	W	C	S	FA	CF	Ad
N	380	678	484	291	-	6
CF-V-0.5%					9	
CF-PY-2%					36	
CF-SO-0.5%					9	

W: Water C: High early strength Portland cement

S: Silica sand No. 7 FA: Fly ash type II CF: Carbon fiber

Ad: High range water reducing admixture



Fig. 2.1 Universal testing machine

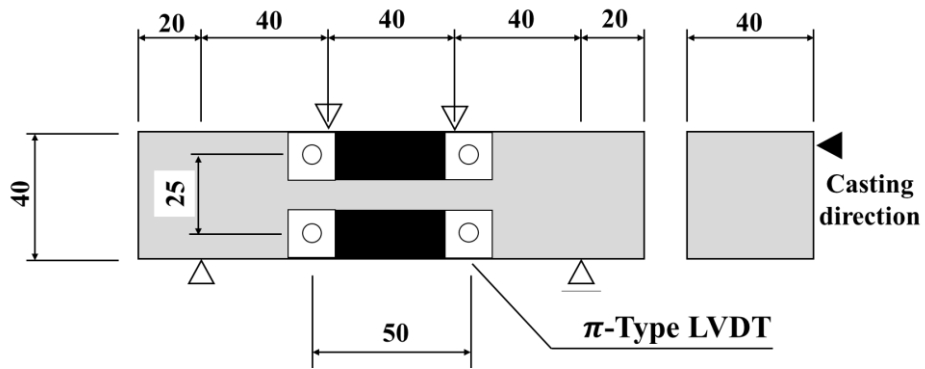


Fig. 2.2 Four-point bending test with 40 mm cross-section

Table 2.2 List of specimens

Specimen	Dimensions	Fiber volume fraction	Quantity
N	Compression: $\phi 50 \times 100$ mm	-	6
CF-V-0.5%		0.5%	6
CF-PY-2%	Bending: $40 \times 40 \times 160$ mm	2%	6
CF-SO-0.5%		0.5%	6

2.1.2 Compression Test Results

Table 2.3 shows a list of average compressive strength and elastic modulus. The average compressive strength and elastic modulus of the four types of specimens are similar. The type of fibers has little effect on the compressive properties. Stress-strain curves of compression test are shown in Fig. 2.3.

Table 2.3 Average compressive strength and elastic modulus

Specimen	Compressive strength (MPa)	Elastic modulus (GPa)
N	44.9	16.0
CF-V-0.5%	48.1	17.2
CF-PY-2%	46.4	17.2
CF-SO-0.5%	52.0	17.1

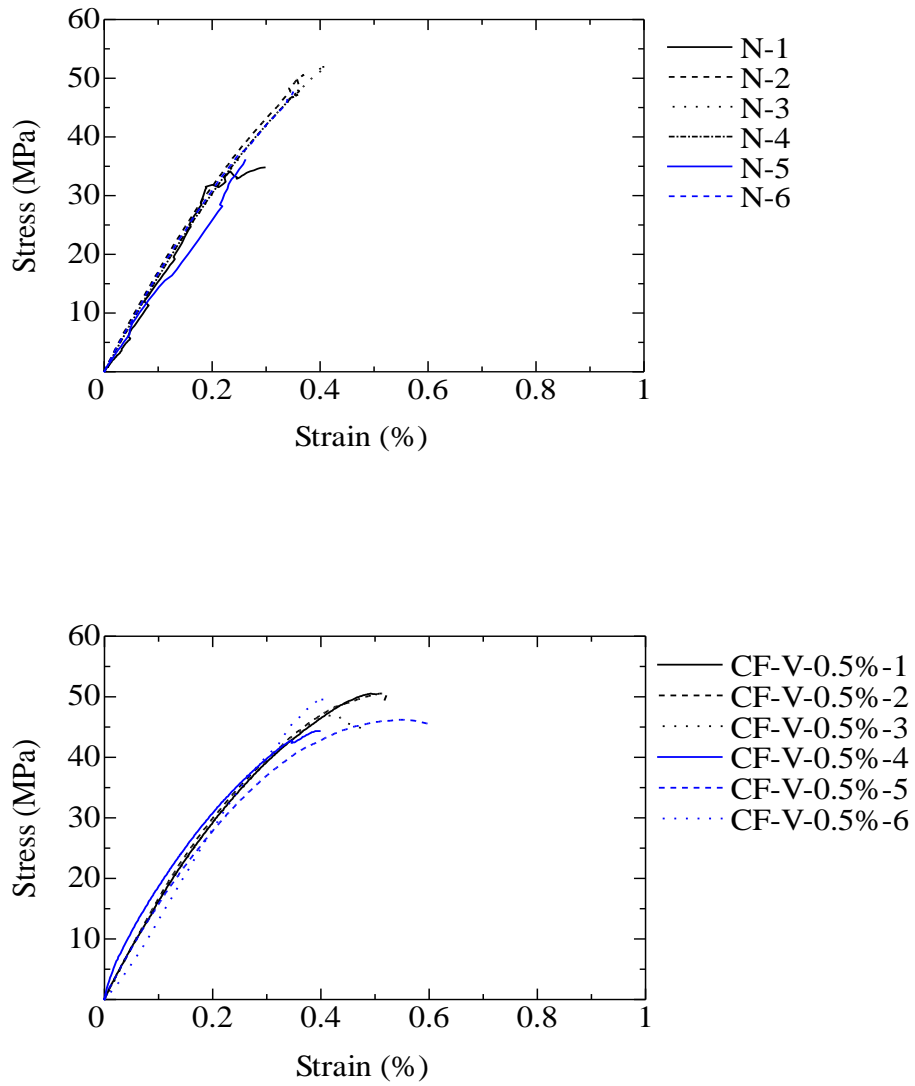


Fig. 2.3 Stress-strain curves of compression test

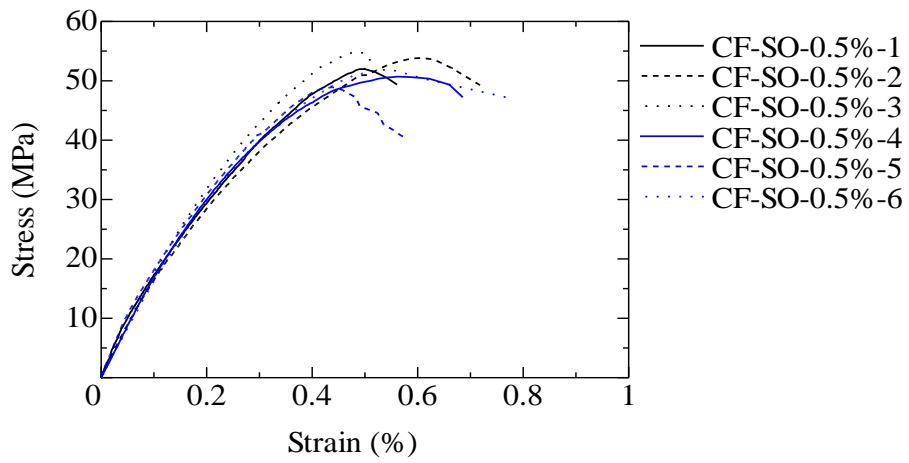
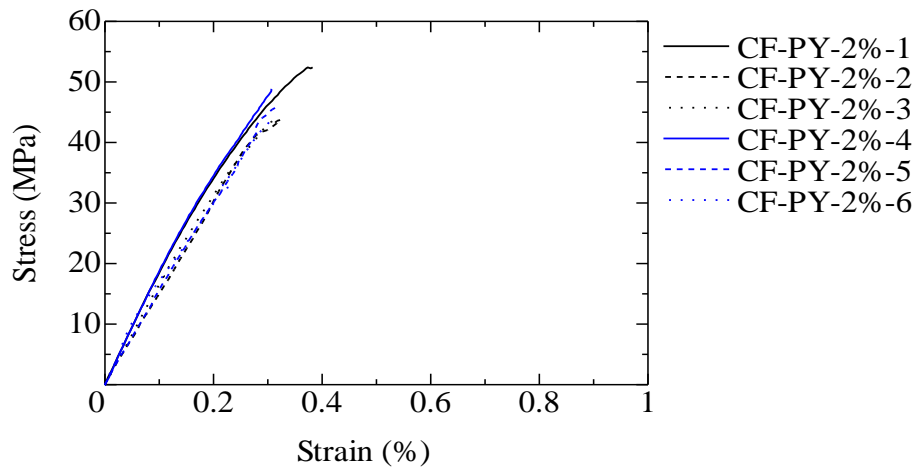


Fig. 2.3 Stress-strain curves of compression test (continued)

2.1.3 Bending Test Results

Typical examples of test pieces after bending test are shown in Fig. 2.4. In all test pieces, one crack took place and failed by opening the crack. In CF-V-0.5% and CF-SO-0.5%, the fibers bridging the crack were observed.

Fig. 2.5 shows the bending moment-curvature curves. In CF-PY-2%, the bending moment increases linearly to the peak. Then the bending moment decreases rapidly. In CF-SO-0.5% and CF-V-0.5%, the bending moment gradually increases after cracking to the peak showing deflection hardening property. After the peak, the bending moment decreases rapidly.

Table 2.4 shows the list of the maximum bending moment and maximum bending stress which is derived as maximum bending moment divided by section modulus. The average maximum bending moment of CF-PY-2% is 0.332 times that of CF-V-0.5%. The average maximum bending moment of CF-SO-0.5% is 0.645 times that of CF-V-0.5%. It is recognized that bridging effect of fibers improves the bending strength and toughness in case of CF-V-0.5% and CF-SO-0.5%.



CF-V-0.5%



CF-PY-2%



CF-SO-0.5%

Fig. 2.4 Bending specimen after loading

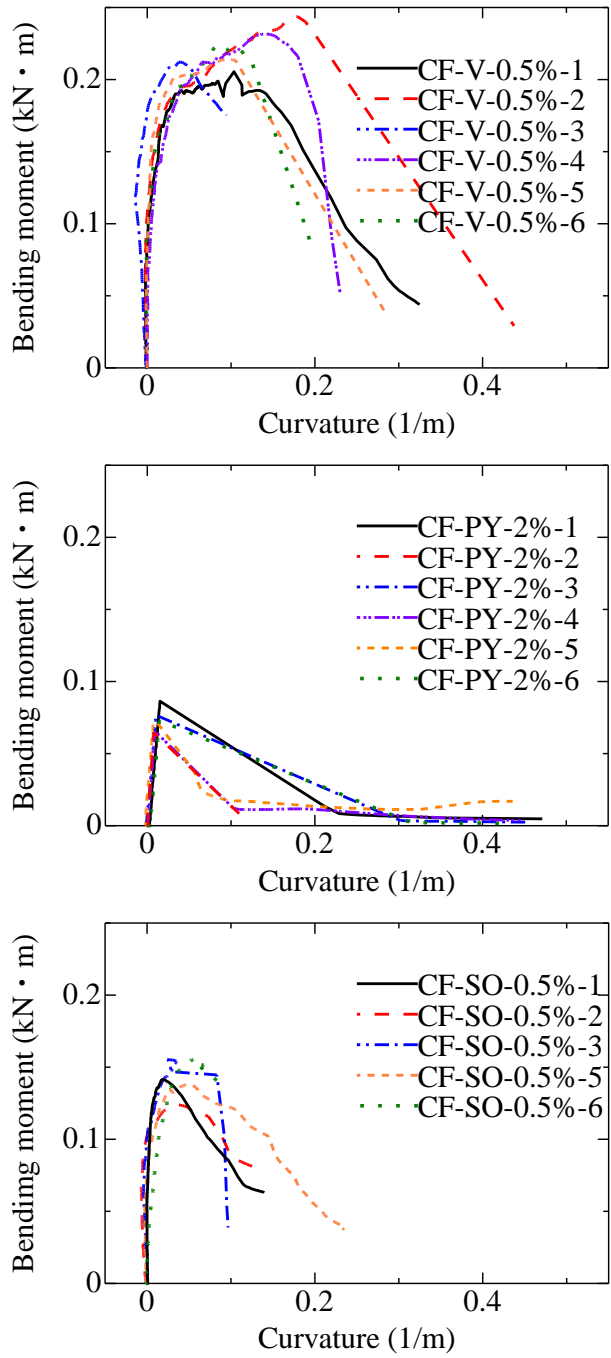


Fig. 2.5 Bending moment-curvature curve

Table 2.4 List of maximum bending moment

Specimen	Maximum bending moment (kN · m)	Maximum bending stress (MPa)
CF-V-0.5%-1	0.192	18.0
CF-V-0.5%-2	0.244	22.9
CF-V-0.5%-3	0.212	19.9
CF-V-0.5%-4	0.232	21.8
CF-V-0.5%-5	0.214	20.1
CF-V-0.5%-6	0.224	21.0
CF-V-0.5%-Avg.	0.220	20.6
CF-PY-2%-1	0.0863	8.1
CF-PY-2%-2	0.0648	6.1
CF-PY-2%-3	0.0765	7.2
CF-PY-2%-4	0.0645	6.0
CF-PY-2%-5	0.0724	6.8
CF-PY-2%-6	0.0730	6.8
CF-PY-2%-Avg.	0.0730	6.8
CF-SO-0.5%-1	0.141	13.2
CF-SO-0.5%-2	0.124	11.6
CF-SO-0.5%-3	0.155	14.5
CF-SO-0.5%-4	0.112	10.5
CF-SO-0.5%-5	0.138	12.9
CF-SO-0.5%-6	0.155	14.5
CF-SO-0.5%-Avg.	0.142	13.3

2.2 Bending Test with 100 mm Cross-section

2.2.1 Experiment Overview

The bending tests with 40 mm cross-section investigate the fabrication of recycled CF-FRCC and the comparisons of bending characteristics between the different types of recycled carbon fiber. As the results, recycled carbon fiber by the solvolysis method shows better behavior rather than that by the pyrolysis method. Therefore, further investigation into the recycled carbon fibers by the solvolysis method is conducted.

The objective of this bending tests with 100 mm cross-section is to investigate the bending characteristics of FRCC with recycled CF by solvolysis methods in specimens by commonly used dimensions. Simultaneously, the test investigates the influence of varying fiber volume fractions in FRCC on flexural performance.

The list of the specimens is shown in Table 2.5 and illustrated in Fig. 2.6. Total 6 specimens for compression test and 10 specimens for four-point bending test were prepared. The used fiber is recycled carbon fiber by the solvolysis method (CF-SO) as same as that used in Section 2.1. The fiber is cut in 10mm long. Table 2.6 shows the mix proportion of FRCC. The fiber volume fraction is set to 0.5% and 0.75%. The fiber is added in two stages to facilitate better fiber dispersion. The specimens were covered with plastic wrap for curing in room environment. The demolding of the test specimens is conducted on the seventh day after casting.

Table 2.5 List of specimens

Specimen	Dimensions	Fiber volume fraction	Number of specimens
CF-SO-0.5%	Compression: $\phi 100 \times 200 \text{ mm}$	0.5%	Compression:3 Bending:5
CF-SO-0.75%	Bending: 100x100x400mm	0.75%	Compression:3 Bending:5

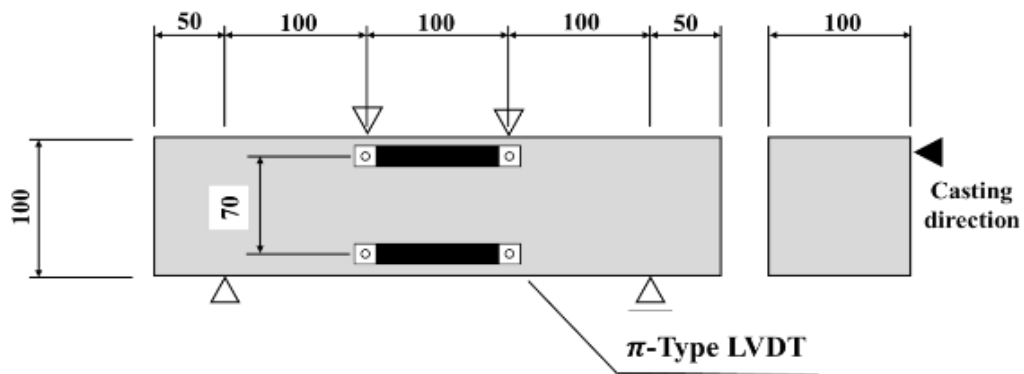


Fig. 2.6 Four-point bending test with 100 mm cross-section

Table 2.6 Mix proportion of FRCC

Specimen	Unit weight(kg/m ³)					
	W	C	S	FA	CF	Ad
CF-SO-0.5%	380	678	484	291	9	6
CF-SO-0.75%					13.5	

W: Water C: High early strength Portland cement

S: Silica sand No. 7 FA: Fly ash type II CF: Carbon fiber

Ad: High range water reducing admixture

2.2.2 Compression Test Results

Table 2.7 shows the results of compression test. FRCC with fiber volume fraction of 0.75% show lower compressive strength than that of 0.5%. Stress-strain curves of compression test are shown in Fig. 2.7.

Table 2.7 Results of compression test

Specimen	Compressive strength (MPa)	Elastic modulus (GPa)
CF-SO-0.5%	40.8	17.2
CF-SO-0.75%	32.4	15.8

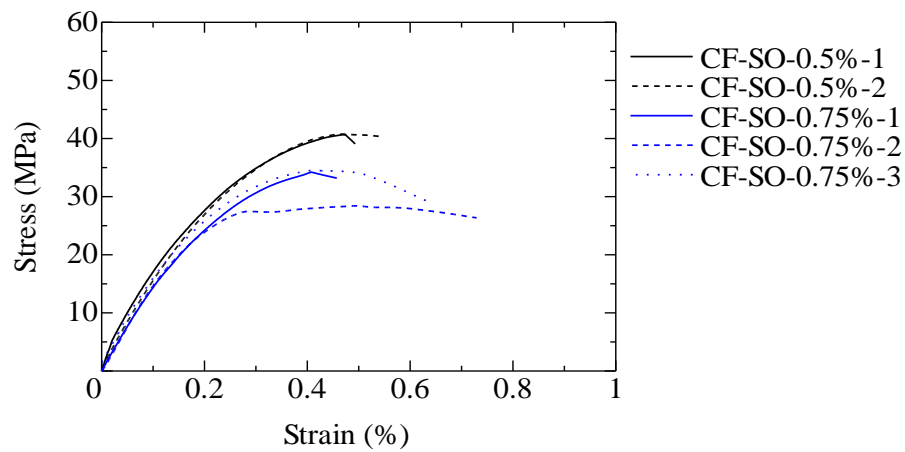


Fig. 2.7 Stress-strain curves of compression test

2.2.3 Bending Test Results

Fig. 2.8 shows the bending moment-curvature curves obtained in the bending test. The deflection hardening property, in which the bending moment increases after first cracking, can be observed in all the specimens. After the peak, the curves showed slight softening branch, and the crack rapidly opened.

Table 2.8 shows the list of the maximum bending moment and maximum bending stress which is derived as maximum bending moment divided by section modulus. The large difference between CF-SO-0.5% and CF-SO-0.75% is not observed.

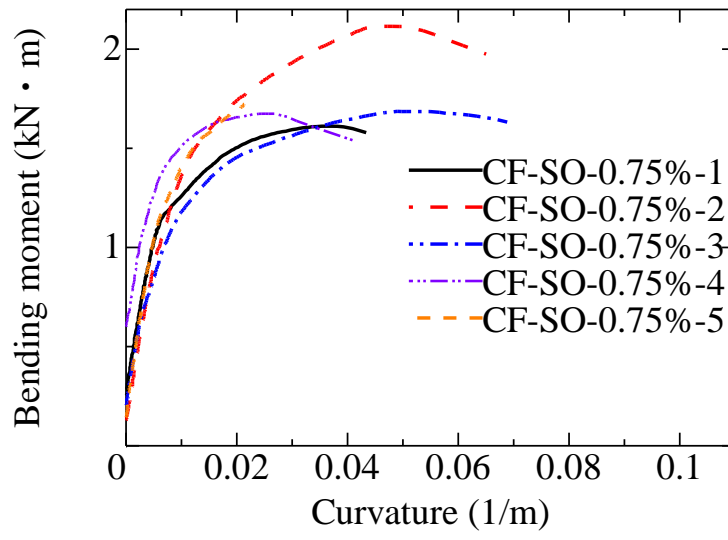
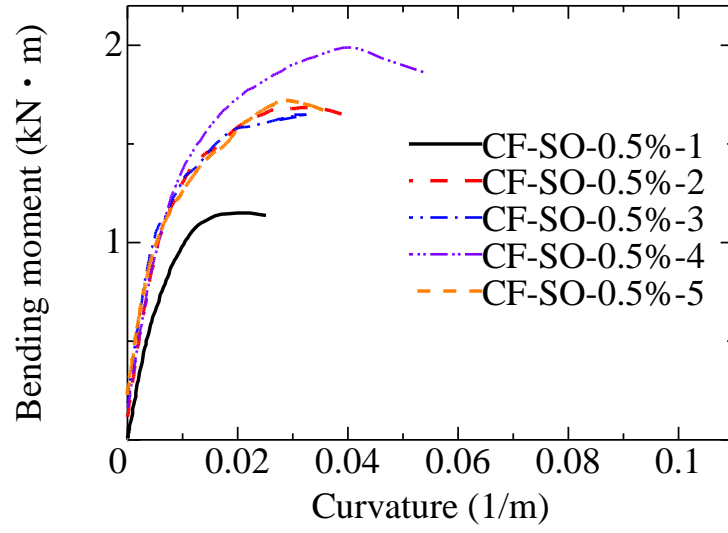


Fig. 2.8 Bending moment-curvature curve

Table 2.8 List of maximum bending moment

Specimen	Maximum bending moment (kN · m)	Maximum bending stress (MPa)
CF-SO-0.5%-1	1.149	6.89
CF-SO-0.5%-2	1.684	10.10
CF-SO-0.5%-3	1.648	9.89
CF-SO-0.5%-4	1.988	11.93
CF-SO-0.5%-5	1.720	10.32
CF-SO-0.5%-Avg.	1.638	9.83
CF-SO-0.75%-1	1.611	9.67
CF-SO-0.75%-2	2.114	12.68
CF-SO-0.75%-3	1.686	10.12
CF-SO-0.75%-4	1.674	10.04
CF-SO-0.75%-5	1.720	10.32
CF-SO-0.75%-Avg.	1.761	10.57

2.3 Experimental Conclusion

The deflection hardening property is observed in FRCC with recycled carbon fiber by the solvolysis method. The maximum bending stress of 100mm cross-section specimens is smaller than that of 40mm specimens. The large difference between CF-SO-0.5% and CF-SO-0.75% is not observed. The suitable fiber volume fraction is considered to be around 0.5% for FRCC with solvolysis method recycled carbon fiber.

Chapter 3 Uniaxial Tension Test

3.1 Experiment Overview

3.1.1 Used Materials

The mix proportion of FRCC is shown in Table 3.1. In this experiment, the recycled carbon fiber by solvolysis method (CF-SO) is used as same as that employed in the bending test. The length of the fiber is also controlled at 10 mm. The fiber volume fraction is set at 0.5%. Table 3.2 shows the mechanical properties of fiber. The fiber is added in two stages to facilitate better fiber dispersion. After casting for one day, transfer the test specimens from the air to water for curing. The specimens are submerged in water at room temperature for six days. The demolding of the test specimens is conducted on the seventh day after casting.

Fig. 3.1 shows the electronic system universal testing machine with a capacity of 200 N. The load speed is set to 1mm/min. The pullout load and head displacement are recorded.

Table 3.1 Mix proportion of FRCC

Specimen	Unit weight(kg/m ³)					
	W	C	S	FA	CF	Ad
CF-SO-0.5%	380	678	484	291	9	6

W: Water C: High early strength Portland cement

S: Silica sand No. 7 FA: Fly ash type II CF: Carbon fiber

Ad: High range water reducing admixture

Table 3.2 Mechanical properties of fiber

Type of fiber	Length (mm)	Diameter (μm)	Tensile strength (MPa)	Elastic modulus (GPa)
CF-SO	10	5	5800	294



Fig. 3.1 Electronic system universal testing machine

3.1.2 Specimens

The list of the specimens is shown in Table 3.3. Total 8 specimens for compression test and 20 specimens for uniaxial tension test were prepared. 7 specimens for uniaxial tension test were damaged and rendered unusable during the demolding process due to the presence of holes in the central position of the specimen. The compression test is carried out by $\phi 100 \times 200$ mm cylinder. For uniaxial tension test, the test section is 30 mm long with a cross-sectional area of 5 mm \times 5 mm, as shown in Fig. 3.2. This size of the test section ensures that the fiber orientation remains consistent, thus eliminating the influence of fiber orientation in this experiment. The mold for the test specimens is shown in Fig. 3.3.

Table 3.3 List of the specimens

Specimen	Dimensions	Fiber volume fraction	Number of specimens
CF-SO-0.5%	Compression: $\phi 100 \times 200$ mm Uniaxial tension test: 5 \times 5 mm cross-section	0.5%	Compression test: 8 Uniaxial tension test: 20

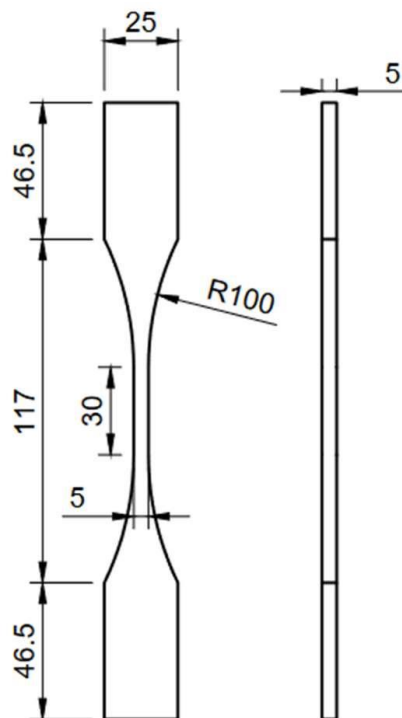


Fig. 3.2 Dimensions of specimen for uniaxial tension test (Unit: mm)



Fig. 3.3 The mold for the test specimens

3.2 Test Results

3.2.1 Compression Test

Table 3.4 shows the results of compression test. Average compressive strength of specimens is 41.9MPa. Average elastic modulus is 16.2GPa. Stress-strain curves of compression test are shown in Fig. 3.4.

Table 3.4 Results of compression test

Specimen	Compressive strength (MPa)	Elastic modulus (GPa)
CF-SO-0.5%-1	46.4	*
CF-SO-0.5%-2	44.3	15.9
CF-SO-0.5%-3	46.3	17.7
CF-SO-0.5%-4	45.3	18.4
CF-SO-0.5%-5	41.0	*
CF-SO-0.5%-6	37.7	15.6
CF-SO-0.5%-7	36.1	14.6
CF-SO-0.5%-8	37.5	15.0
Average	41.9	16.2

*: Strain measurement was not carried out properly.

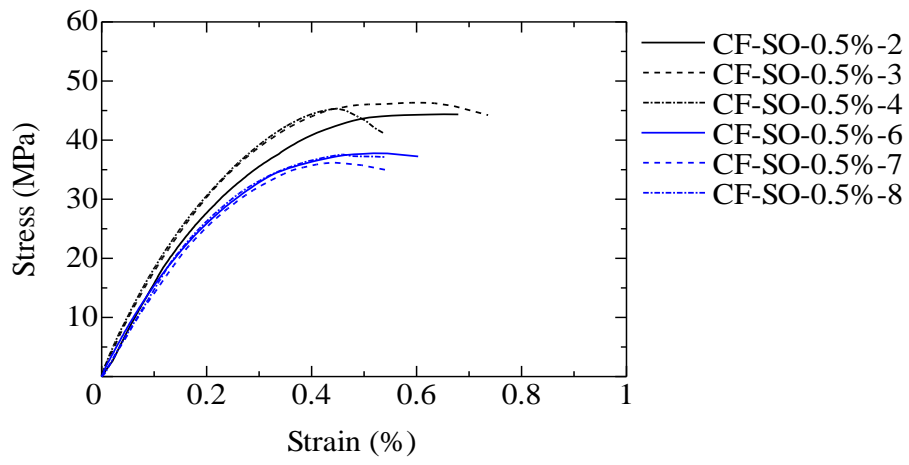


Fig. 3.4 Stress-strain curves of compression test

3.2.2 Uniaxial Tension Test

Fig. 3.5 illustrate the results of the uniaxial tension test. Tension load and head displacement relationship for each specimen is presented. Fig. 3.6 shows the photos of specimens after loading. During the loading process, a crack formed in the central position of the specimens. Most of the fiber was ruptured. The maximum load values and their corresponding displacements are presented in Table 3.5. The average value of the maximum load is 108.2 N. The tensile strength ranging from 2.32 N/mm² to 6.64 N/mm², and the average tensile strength is 4.32 N/mm².

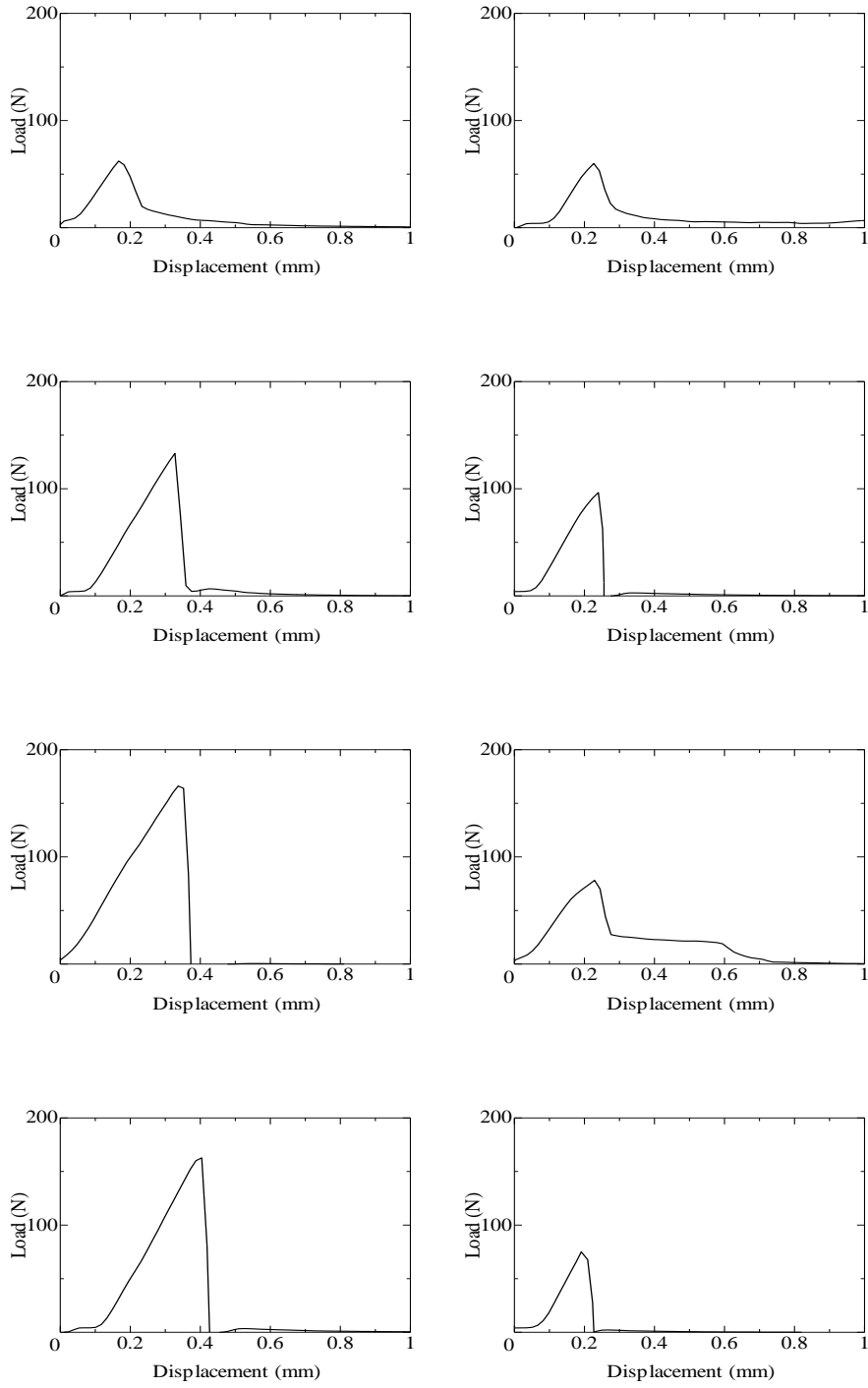


Fig. 3.5 Tensile load-head displacement relationship

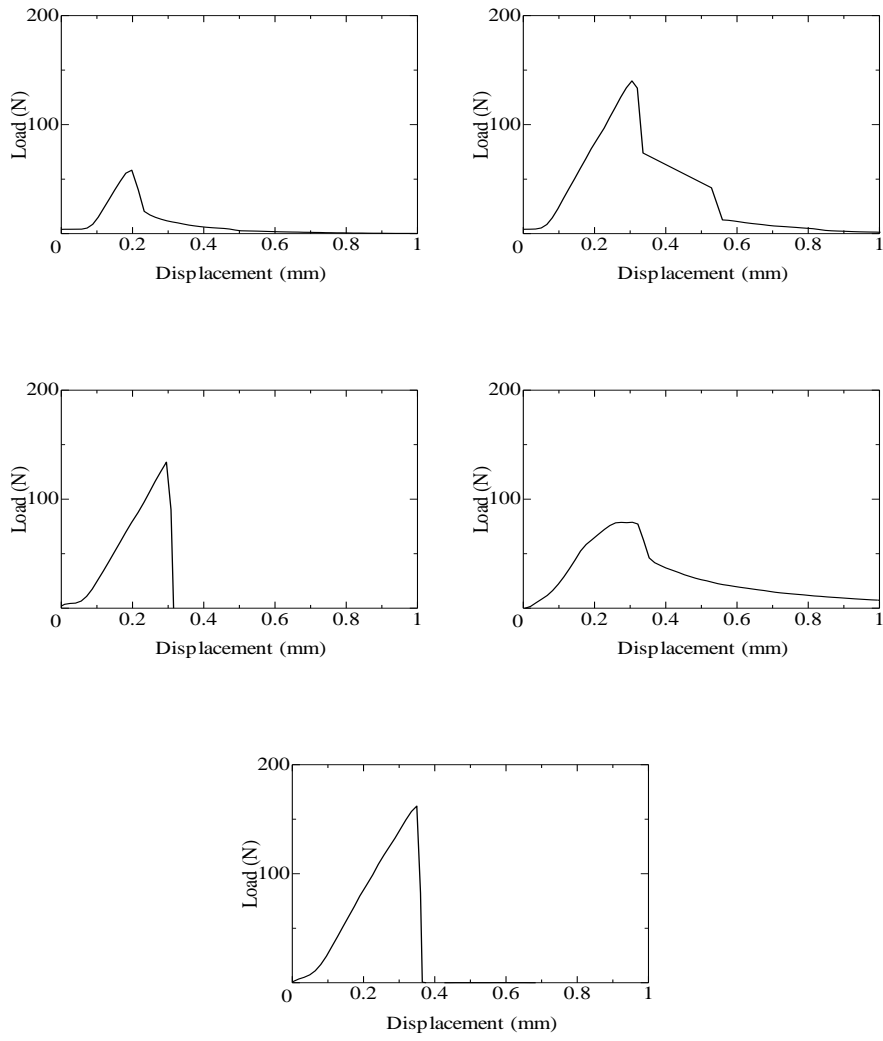


Fig. 3.5 Tensile load-head displacement relationship (continued)

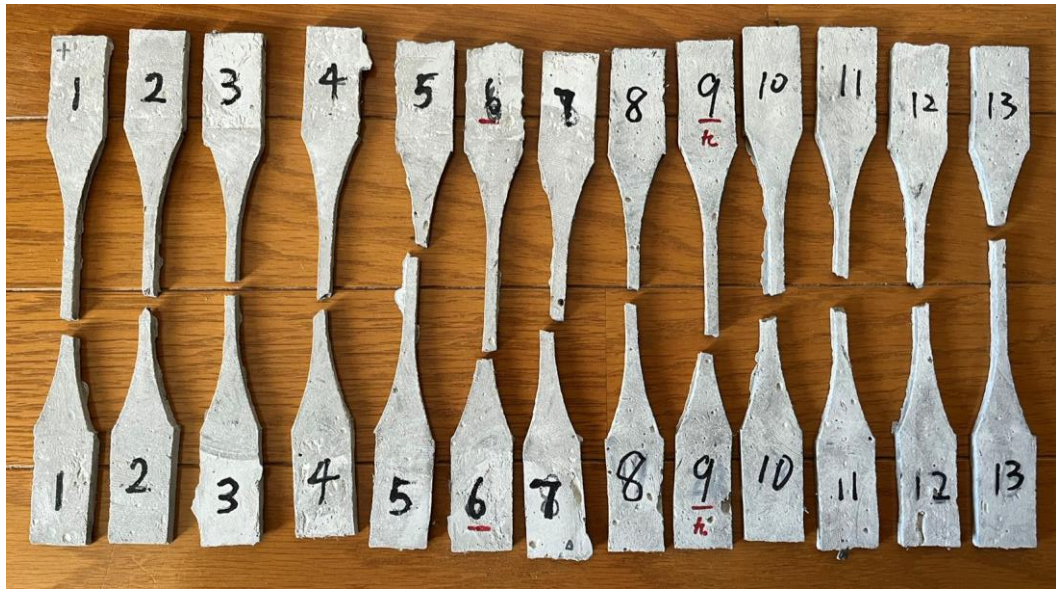


Fig. 3.6 Photos of specimens after loading

Table 3.5 Results of the uniaxial tension test

Specimen	Maximum load (N)	Corresponding displacement (mm)	Tensile strength (N/mm ²)
CF-SO-0.5%-1	62.2	0.166	2.48
CF-SO-0.5%-2	59.8	0.226	2.39
CF-SO-0.5%-3	132.9	0.327	5.31
CF-SO-0.5%-4	96.3	0.239	3.85
CF-SO-0.5%-5	166.2	0.336	6.64
CF-SO-0.5%-6	78.1	0.229	3.12
CF-SO-0.5%-7	162.7	0.404	6.51
CF-SO-0.5%-8	75.0	0.191	3.00
CF-SO-0.5%-9	58.2	0.197	2.32
CF-SO-0.5%-10	140.1	0.305	5.60
CF-SO-0.5%-11	133.9	0.295	5.35
CF-SO-0.5%-12	78.8	0.306	3.15
CF-SO-0.5%-13	162.0	0.349	6.48
Average	108.2	0.275	4.32

Chapter 4 Modeling of Bridging Law

4.1 Bridging Law

The bridging law (tensile stress - crack width relationship) is calculated by the summation of forces carried by individual bridging fibers [1].

The number of fibers in the uniaxial tension specimens can be calculated by Equation (4.1).

$$N_f = V_f \times \frac{A_m}{A_f} \quad (4.1)$$

Where,

N_f : calculated number of fibers

V_f : fiber volume fraction

A_m : cross-sectional area of the specimen

A_f : cross-sectional area of fiber

In this experiment, the fiber volume fraction is set to 0.5%. Cross-sectional area of the specimen is 5×5 mm. The diameter of the fiber is 5 μm. Therefore, the number of fibers in the cross-section is calculated to be 6366.

Since the uniaxial tension test specimens exclude the influence of fiber orientation, the only factor affecting fiber bridging behavior is the embedded length of the individual fibers. The calculated bridging force can be obtained by Equation (4.2).

$$P_{bridge} = \sum_{l_b \leq l_f/2} P(l_b) \quad (4.2)$$

Where,

P_{bridge} : bridging force

$P(l_b)$: pullout force of individual fiber

l_b : embedded length

l_f : length of fiber

According to the experimental data from the uniaxial tension tests, the individual fiber bridging model can be obtained reversibly using Equation (4.2). Fig. 4.1 illustrates the individual fiber bridging model, which is the bi-linear model. Based on the average value of the maximum load, the peak value for P_{bridge} has been determined to be 108.2 N. The crack width corresponding to the peak load is determined from the average experimental data and has been measured to be 0.25 mm. Table 4.1 illustrates the spreadsheet software (Excel) procedure for calculating the bridging law. The first row and the first column represent the crack width and the embedded length of the fiber, respectively. When the crack width exceeds the embedded length, the fiber is considered to be fully pulled out, and the tensile force becomes 0 N. The data within the table represents the tensile force of an individual fiber. The last column represents the sum of tensile forces of all fiber across the entire cross-section, which is equal to the applied load. As a result of finding the characteristic points of the bilinear model to match the maximum load and displacement of the uniaxial tension test results, the maximum tensile load of the individual fiber is 0.0177 N and the corresponding crack width is 0.25 mm as shown in Fig. 4.1. The calculation result of bridging law is shown

in Fig. 4.2. The load becomes to zero when crack width becomes equal to half of its total length.

Table 4.1 Calculation procedure of bridging law

Crack Width (mm)	0.1	0.2	0.3	...	4.8	4.9	5	Load (N)
0	0.00	0.00	0.00	...	0.00	0.00	0.00	0.00
0.05	0.00	0.00	0.00	...	0.00	0.00	0.00	22.54
0.1	0.01	0.01	0.01	...	0.01	0.01	0.01	45.09
0.15	0.00	0.01	0.01	...	0.01	0.01	0.01	66.28
0.2	0.00	0.01	0.01	...	0.01	0.01	0.01	88.37
0.25	0.00	0.00	0.02	...	0.02	0.02	0.02	108.21
...
4.75	0.00	0.00	0.00	...	0.00	0.00	0.00	0.36
4.8	0.00	0.00	0.00	...	0.00	0.00	0.00	0.28
4.85	0.00	0.00	0.00	...	0.00	0.00	0.00	0.14
4.9	0.00	0.00	0.00	...	0.00	0.00	0.00	0.09
4.95	0.00	0.00	0.00	...	0.00	0.00	0.00	0.02
5	0.00	0.00	0.00	...	0.00	0.00	0.00	0.00

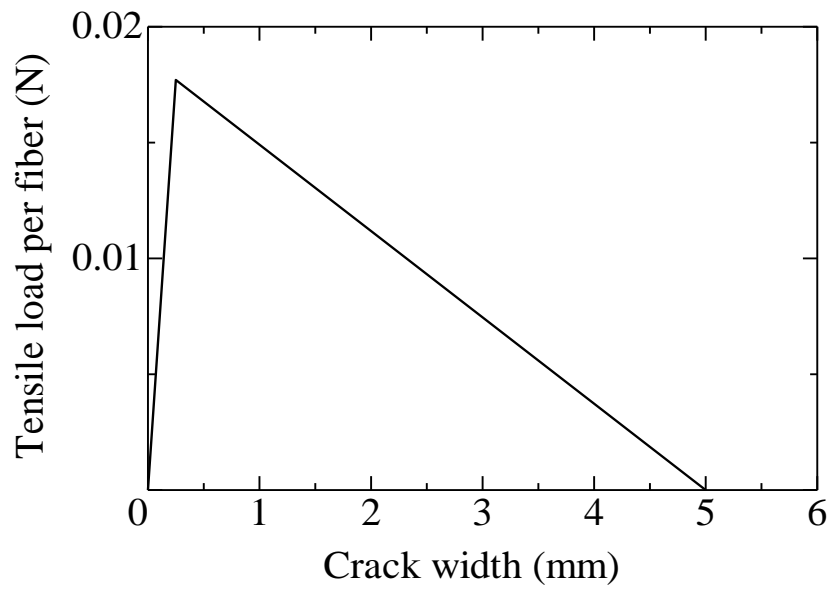


Fig. 4.1 Individual fiber bridging model

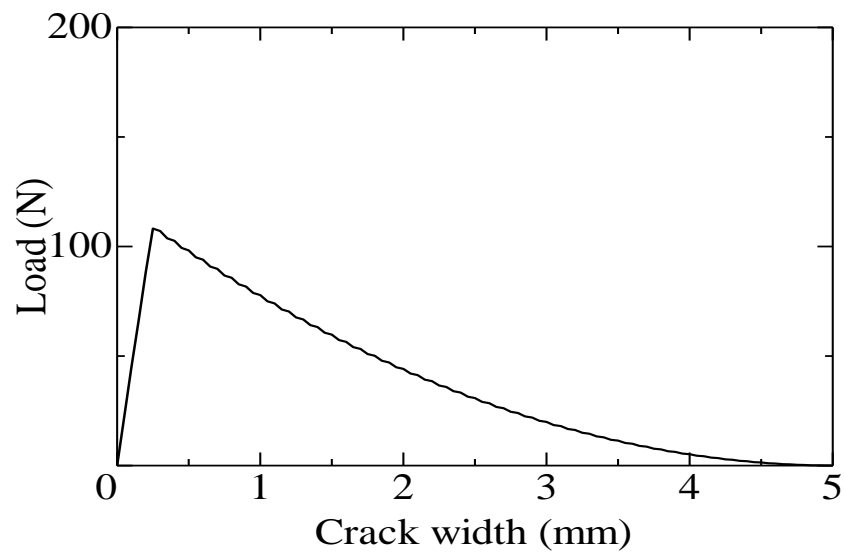


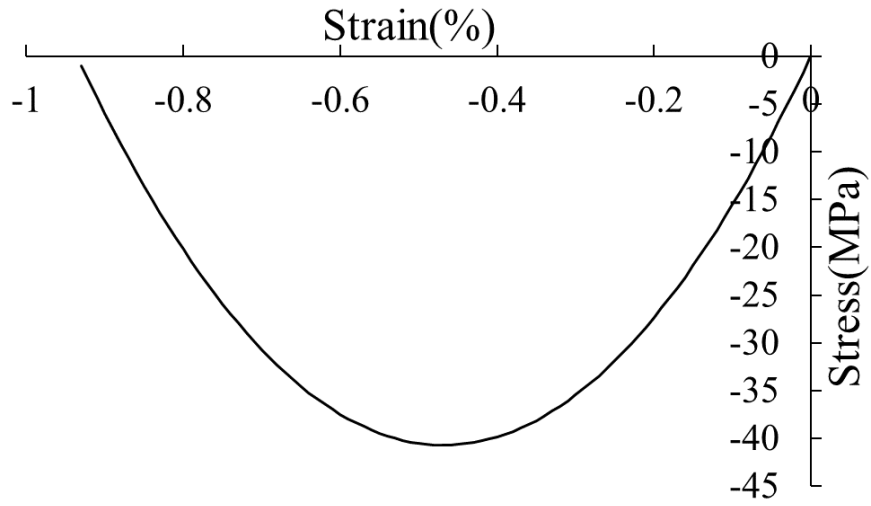
Fig. 4.2 Calculation result of bridging law

4.2 Section Analysis for Bending Test

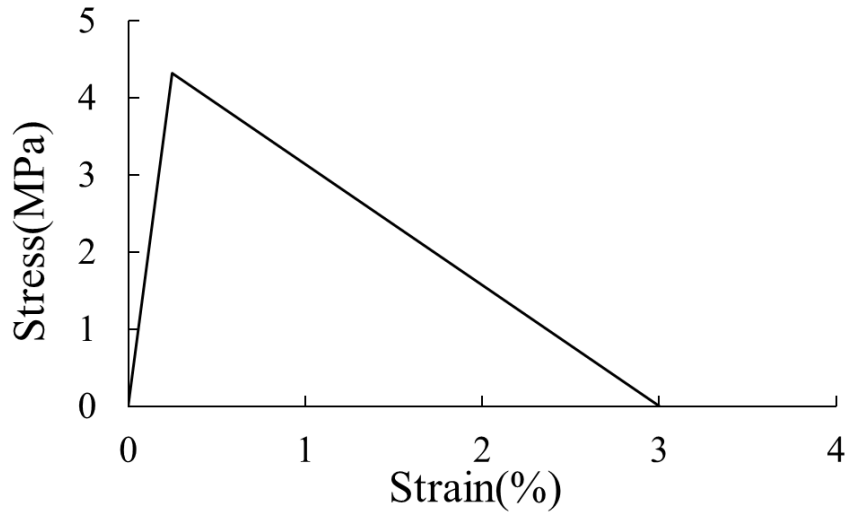
Section analysis is conducted to compare the tensile characteristics of FRCC. The stress-strain model in tension side is derived based on the bridging law depicted in Fig. 4.2 and the data from compression tests are used in compression side, as presented in Fig. 4.3. The tension side is represented by the bi-linear model, while the compression side is modelled by the parabolic model. For tension side, stress is obtained by dividing the load by the cross-sectional area, while strain is determined by dividing the crack width from the bridging law by the pure bending length of the bending specimen, which is 100 mm. The peak value of stress is obtained by dividing the maximum load of 108.2N from Fig. 4.2 by the cross-sectional area of 25 mm², resulting in 4.328 MPa. The corresponding peak strain is 0.25%. The ultimate strain at which stress drops to 0 MPa is 3%, as inferred from the descending branch of the curve in Fig. 4.2.

Table 4.2 shows the list of maximum bending moment by experimental and calculated values. The calculated maximum bending moment is 0.95 times the experimental data, showing a close agreement.

Fig. 4.4 shows stress distributions in the cross-section of the specimen at the maximum bending moment. The horizontal axis indicates the stress of FRCC, showing compression in the left (negative) and tension in the right (positive).



(a) compression side



(b) tension side

Fig. 4.3 Stress-strain model for section analysis

Table 4.2 List of maximum bending moment

Specimen	Experiment	Section analysis	
	Max. bending moment (kN·m)	Max. bending moment (kN·m)	Ratio between experimental and calculated values
CF-SO-0.5%	1.638	1.561	0.95

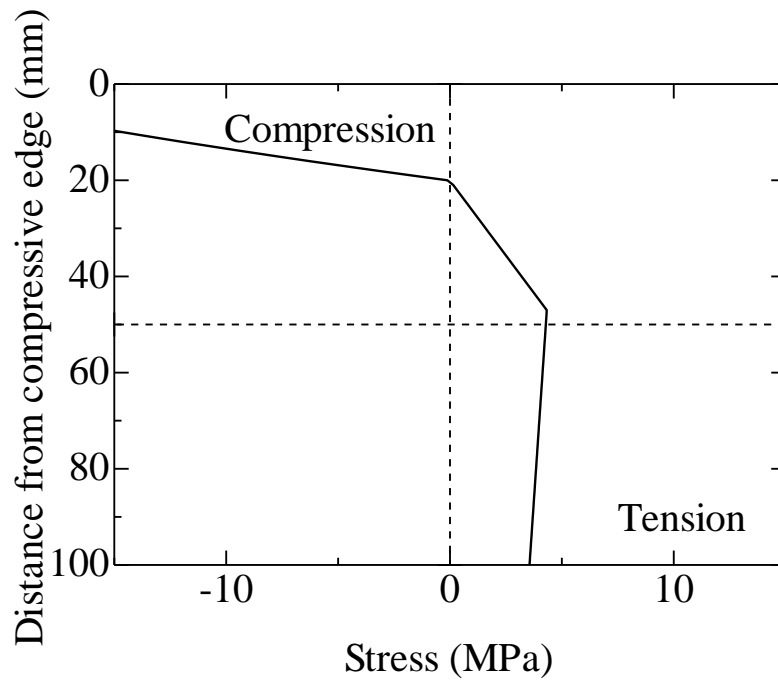


Fig. 4.4 Stress distribution in cross-section at the maximum moment

Chapter 5 Conclusion

This study focuses on the effective utilization of recycled carbon fibers and their impact on the tensile characteristics of FRCC. Various recycled carbon fiber is employed in four-point bending tests, and further uniaxial tension tests are conducted on recycled carbon fibers by the solvolysis method. Based on the results of experiment and the calculation of the bridging law, the following conclusions are drawn:

- (1) Based on the results of the bending tests, recycled carbon fiber by the solvolysis method exhibits better mechanical performance compared to other fibers.
- (2) The deflection hardening property is observed in FRCC with recycled carbon fiber by the solvolysis method. The suitable fiber volume fraction is considered to be around 0.5% for FRCC with solvolysis method recycled carbon fiber.
- (3) The bridging law, derived from the data obtained in uniaxial tension tests, serves as the subject for further exploration of the tensile characteristics of FRCC by solvolysis method recycled carbon fiber.
- (4) Section analysis under bending condition is conducted using the bridging law. The calculated maximum bending moment is 0.95 times the experimental data, demonstrating a close agreement.

Acknowledgements

I would like to express my deepest gratitude to those who have contributed to the completion of this research.

First and foremost, I extend my sincere appreciation to my academic supervisor, Prof. Toshiyuki Kanakubo, for his invaluable guidance and unwavering support throughout this research project. His expertise, patience, and insightful feedback have been instrumental in shaping the direction of this work.

I am grateful to Professor Akira Yasojima and Professor Takashi Matsushima for their valuable suggestions that have enriched the quality of this research. Their expertise in the field has been a source of inspiration. Also, gratitude is extended to technical staff Mr. Kojima for providing valuable assistance during the experimental process.

Special thanks go to Mr. Hang Zhang, Mr. Hideto Sasaki and Mr. Weichao Tian, whose collaboration and input significantly contributed to the success of this project. The exchange of ideas and collective efforts have undoubtedly enhanced the depth and breadth of our findings.

Also, I would like to acknowledge the MIRAI KASEI INC. and Toray Industries, Inc for providing the recycled carbon fiber.

Reference

[1] Toshiyuki Kanakubo, Masaru Miyaguchi, Kohei Asano: Influence of Fiber Orientation on Bridging Performance of Polyvinyl Alcohol Fiber-Reinforced Cementitious Composite, Materials Journal, American Concrete Institute, Vol.113, No.2, pp.131-141, 2016.3

[2] 炭素繊維強化プラスチック(CFRP) のリサイクルの現状と課題, 廃棄物資源循環学会, Vol. 29, No. 2, pp. 133- 141, 2018

[3] Houssam A. Toutanji, Tahar El-Korchi, R.Nathan Katz: Strength and reliability of carbon-fiber-reinforced cement composites, Cement and Concrete Composites, Vol. 16, No. 1, pp.15-21, 1994

[4] Hideto Sasaki, Sicong Li, Toshiyuki Kanakubo: Fabrication of Fiber-Reinforced Cementitious Composite with Recycled Carbon Fiber, Japan Society of Civil Engineers 2023 Annual Meeting, V-751, 2023.9